DALTON
FULL PAPER

Can aromatic interactions control the coordination geometry of zinc complexes? Structural evidence and a possible mechanism for the conversion of trigonal-bipyramidal to octahedral compounds

Nicole Niklas,[a] Olaf Walter,[b] Frank Hampel[c] and Ralf Alsfasser*[a]

[a] *Institute of Inorganic Chemistry, University of Erlangen-Nürnberg, Egerlandstr. 1, D-91058 Erlangen, Germany. E-mail: alsfasser@chemie.uni-erlangen.de*
[b] *ITC-CPV, Forschungszentrum Karlsruhe, Postfach 3640, D-76021 Karlsruhe*
[c] *Institute of Organic Chemistry, University of Erlangen-Nürnberg, Henkestrasse 42, D-91054 Erlangen*

Received 29th April 2002, Accepted 4th July 2002
First published as an Advance Article on the web 8th August 2002

Aromatic interactions are well known to participate in the structural stabilization of biological macromolecules. We have utilized this motif as an unconventional new means to control the stereochemistry of synthetic zinc complexes. The aromatic amino acid L-phenylalanine has been applied as a building block in the chiral ligand bpaAc–Phe–OMe (*N*,*N*-bis(2-picolyl)aminoacyl-(*S*)-phenylalanine-methylester). Zinc(II) complexes of this ligand are always trigonal–bipyramidal in the solid state. This is confirmed by the X-ray structures of $[(bpaAc–Phe–OMe)Zn(OTf)]^+$ (**1b**, OTf = Triflate), $[(bpaAc–Phe–OMe)Zn(H_2O)]^{2+}$ (**2b**), and $[(bpaAc–Phe–OMe)Zn(pz)]^{2+}$ (**3b**). In contrast, the octahedral complexes $[(bpaAc–Gly–OEt)Zn(pz)(OTf)]^+$ (**3a**) and $[(bpaAc–Gly–OEt)Zn(N\text{-Meim})(H_2O)]^{2+}$ (**4a**) have been obtained with the related glycine derived ligand bpaAc–Gly–OEt. A comparison with the five-coordinate structures of $[(bpaAc–Gly–OEt)Zn(OTf)]^+$ (**1a**) and $[(bpaAc–Gly–OEt)Zn(Cl)]^+$ (**5**) allows an appreciation of effects brought about by (1) the coligand (chloride, triflate, pyrazole, *N*-methylimidazole) and (2) the non-coordinating amino acid side chain (benzyl in bpaAc–Phe–OMe). It is shown that the pyrazole complex **3b** adopts an unusual tense five-coordinate geometry which is stabilized by weak aromatic interactions. The structure represents an analogue of the possible transition state between five-coordinate trigonal-bipyramidal and six-coordinate octahedral complexes in our series.

Introduction

The fascinating structural and catalytic properties of metalloenzymes have stimulated the design of synthetic polydentate ligands which mimic the coordination environment of metal ions in proteins. A major concern in such biomimetic studies is the stabilization of unusual coordination numbers and geometries which are characteristic for enzymes.[1,2] Among the ligands employed those with tripodal $A(N_3)$,[3–9] mixed $A(N_2O)$[10–14] and $A(N_2S)$[15–18] donor sets are most popular ("A" is the bridgehead atom, *e.g.* N, P, B, or C). However, despite the progress made and the impressive number of ligands synthesized it remains a challenge to achieve the desired control over the coordination environment of metal complexes.

Two different stabilizing effects have been used to model zinc containing enzymes.[19] Bulky substituents have been introduced to shield the metal center in tetrahedral trispyrazolylborato complexes $[B(N_3)Zn–X]$.[20–22] The same strategy has enabled the groups of Ogawa[23] and Vahrenkamp[24] to synthesize unusual trigonal-bipyramidal complexes of the type $[N(N_2O)Zn–OH_2]$. A different approach has been taken by Kimura *et al.* who have stabilized an $[N(N_2O)Zn–OH_2]$ complex by the rigid geometry of a tetraaza macrocycle.[25]

We have recently reported the synthesis and some complexes of the amino acid derived ligands bpaAc–Phe–OMe and bpaAc–Gly–OEt (bpaAc = *N*,*N*-bis(2-picolyl)aminoacyl, Phe = (*S*)-phenylalanine, Gly = glycine) shown in Scheme 1.[26] Our $N(N_2O)$ ligand framework bpaAc is flexible and readily forms both, five- and six-coordinate species.[27,28] Furthermore, one would not expect the benzyl group of bpaAc–Phe–OMe to form a rigid hydrophobic pocket. Thus, none of the two stabilizing effects described above can occur. However, the X-ray structure of the complex $[(bpaAc–Phe–OMe)Zn(H_2O)]^{2+}$ (**2b**) suggests that aromatic interactions may help to stabilize a trigonal-bipyramidal coordination sphere.[26,28]

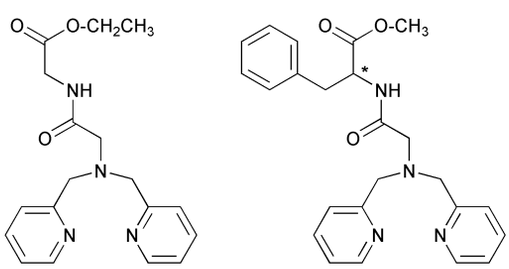

Scheme 1 Structures of the ligands bpaAc–Gly–OEt and bpaAc–Phe–OMe.

With the structural characterization of pyrazole and *N*-methylimidazole complexes we are now able to verify this proposal. The complexes $[(bpaAc–Phe–OMe)Zn(pz)]^{2+}$ (**3b**, pz = pyrazole) and $[(bpaAc–Gly–OEt)Zn(pz)(OTf)]^+$ (**3a**, OTf = triflate) provide the first clear example for the stabilization of trigonal-bipyramidal over octahedral coordination by aromatic interactions. An interesting additional aspect is revealed. Our complete family of new and already published structures enables us to formulate the first reaction trajectory for the important conversion of five- to six-coordinate zinc complexes.

Results

Synthesis

Scheme 2 shows the ligand exchange reactions performed. Starting materials were the triflate (OTf) complexes [(bpaAc–

DOI: 10.1039/b204125c

This journal is © The Royal Society of Chemistry 2002

Gly–OEt)Zn(OTf)]$^+$ (**1a**) and [(bpaAc–Phe–OMe)Zn(OTf)]$^+$ (**1b**).[26] Both cations are trigonal-bipyramidal. The crystal structure of **1b** is described below. If solutions of **1a** and **1b** are not rigorously dry, the compounds always exist in equilibrium with their aquo analogs **2a** and **2b**. We will indicate this by writing **1a**,**b**/**2a**,**b** when reactions of the compounds are discussed. The five-coordinate structure of **2b** has been established by X-ray crystallography.[26] Unfortunately we were not able to crystallize the corresponding glycine derivative **2a**. Based on elemental analysis or spectroscopic data it is not possible to distinguish between the five- and six-coordinate geometries indicated in Scheme 2. Reactions of **1a**,**b**/**2a**,**b** with one equivalent of the respective aromatic heterocycle pyrazole (pz) and *N*-methylimidazole (*N*-Meim) produce the complexes **3a**,**b** (pz) and **4a**,**b** (*N*-Meim). The complexes **3a** and **4a** containing the glycine ligand bpaAc–Gly–OEt are octahedral. This has been confirmed by the X-ray structure analyses of **3a** and **4a**. In contrast, the complexes **3b** and **4b** of the phenylalanine ligand bpaAc–Phe–OMe are trigonal-bipyramidal. For the pyrazole complex **3b** this has been demonstrated by X-ray crystallography. The analogous *N*-methylimidazole complex **4b** has been characterized by C,H,N-elemental analysis and NMR spectroscopy. All data are similar to those of **3b** suggesting a similar five-coordinate structure.

Crystal structures

In this paragraph we describe the new crystal structures of **1b**, **3a**, **3b**, and **4a**. Table 2 (see Experimental) contains details of the structure determinations. Bond lengths and angles of all complexes are compared in Table 1. Included are data of the complexes **1a**, **2b**[26] and the trigonal-bipyramidal chloro complex [(bpaAc–Gly–OEt)ZnCl]$^+$ (**5**)[27] for comparison. Generally, the observed values are typical for zinc complexes of tetradentate ligands derived from tris[(2-pyridyl)methyl]amine.[28–31] However, several subtle changes are observed in our series. These map a well defined stereochemical transition from trigonal-bipyramidal to octahedral geometries. We mainly focus on this aspect and on the orientation of the benzyl substituent in bpaAc–Phe–OMe complexes. The following paragraphs are organized accordingly.

Fig. 1 shows the structure of the achiral trigonal-bipyramidal monocations [(bpaAc–Gly–OEt)Zn(OTf)]$^+$ (**1a**) and [(bpaAc–Gly–OEt)Zn(Cl)]$^+$ (**5**). The three chiral zinc complexes [(bpaAc–Phe–OMe)Zn(OTf)]$^+$ (**1b**), [(bpaAc–Phe–OMe)-Zn(H_2O)]$^{2+}$ (**2b**), and [(bpaAc–Phe–OMe)Zn(pz)]$^{2+}$ (**3b**) are shown in Fig. 2. Finally, the structures of the two octahedral cations [(bpaAc–Gly–OEt)Zn(pz)(OTf)]$^+$ (**3a**) and [(bpaAc–Gly–OEt)Zn(*N*-Meim)(H_2O)]$^{2+}$ (**4a**) are contained in Fig. 3.

It was difficult to isolate the triflate complex [(bpaAc–Phe–OMe)Zn(OTf)]$^+$ (**1b**, Fig. 2) since it is extremely moisture sensitive. We have obtained only a few crystals containing **1b** from a sample which largely consisted of the corresponding aquo complex **2b**. The structure refined best assuming the constitution {([(bpaAc–Phe–OMe)Zn(OTf)][OTf])$_{0.57}$([(bpaAc–Phe–OMe)(H_2O)Zn][OTf]$_2$·H_2O)$_{0.43}$} (57% **1b** + 43% **2b**·(H_2O)). Both [(bpaAc–Phe–OMe)Zn]$^{2+}$ moieties overlap and an oxygen

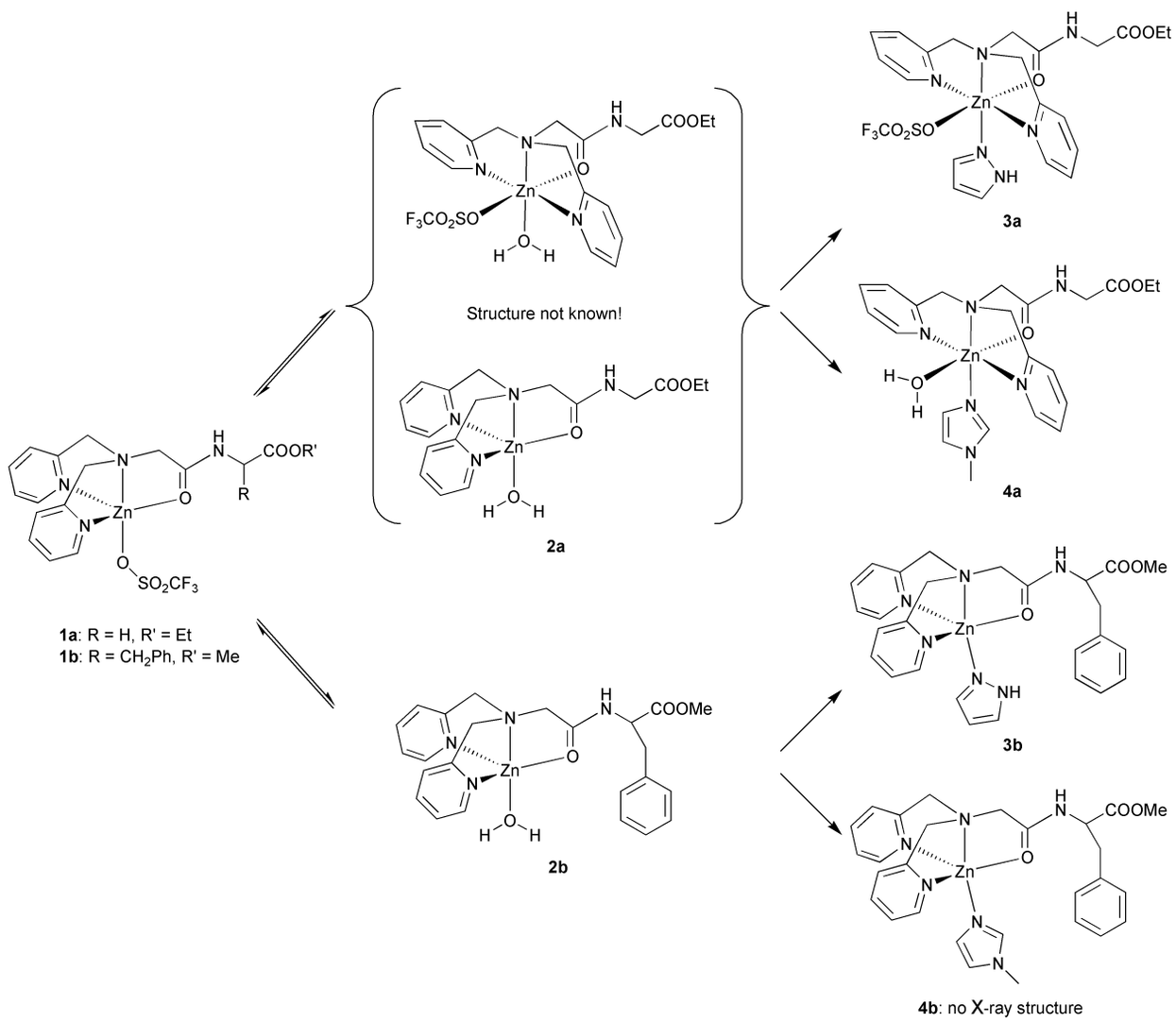

Scheme 2 Zinc complexes of the ligands bpaAc–Gly–OEt and bpaAc–Phe–OMe.

Table 1 Comparison of selected angles [°] and bond lengths [pm] of all complexes characterized by X-ray structure analysis

	5	1a	1b	2b	3b	3a	4a
N1–Zn–N2	78.27(19)	80.18(8)	79.84(14)	80.87(11)	78.44(6)	78.82(19)	77.70(13)
N1–Zn–N3	77.16(17)	80.32(8)	80.05(17)	79.48(12)	78.42(7)	77.59(19)	77.47(14)
N1–Zn–O1	76.35(16)	80.68(7)	80.70(12)	78.45(10)	76.13(5)	78.16(16)	78.05(13)
N1–Zn– L (*trans* to N1)	177.14(12)	176.93(8)	178.52(16)	170.40(13)	165.42(6)	167.51(18)	167.74(16)
N2–Zn–N3	113.74(18)	121.80(8)	119.39(18)	123.42(13)	119.95(7)	151.3(2)	151.92(14)
O1–Zn–N2	114.60(17)	113.13(8)	111.12(15)	113.12(11)	112.80(6)	97.08(17)	88.52(13)
O1–Zn–N3	117.46(18)	116.84(8)	120.93(15)	113.91(11)	113.97(6)	93.78(17)	98.94(13)
O1–Zn–L (*trans* to N1)	100.81(12)	99.29(9)	98.43(15)	92.52(12)	89.38(6)	89.47(17)	89.98(14)
N2–Zn–L (*trans* to N1)	102.86(14)	97.06(8)	99.41(17)	105.96(15)	106.38(7)	104.7(2)	99.56(14)
N3–Zn–L (*trans* to N1)	104.60(13)	102.36(8)	101.4(2)	101.59(15)	109.58(7)	101.8(2)	107.42(15)
O1–Zn–O4		—	—	—	—	174.28(15)	174.81(14)
N2–Zn–O4		—	—	—	—	86.10(17)	87.24(16)
N3–Zn–O4						85.53(17)	83.50(15)
N1–Zn–O4		—	—	—	—	107.18(16)	98.11(15)
O4–Zn–N5		—	—	—	—	85.13(17)	93.66(17)
Zn–N1	226.1(5)	218.83(19)	222.0(3)	218.9(3)	226.42(16)	228.7(5)	228.3(4)
Zn–N2	204.7(5)	203.9(2)	204.2(4)	204.6(3)	205.12(17)	205.2(5)	211.1(3)
Zn–N3	207.1(5)	206.0(2)	204.3(6)	205.7(3)	205.87(18)	206.5(5)	209.4(4)
Zn–O1	207.9(4)	201.97(18)	201.1(3)	205.4(2)	207.56(13)	210.7(4)	212.7(3)
Zn– L (*trans* to N1)	225.25(17)	201.45(18)	203.0(4)	199.0(3)	202.94(16)	205.6(5)	204.1(4)
Zn–O4		—	—	—	—	228.7(4)	218.1(4)

Table 2 Details of crystal structure analyses

Compound	1b	3a	3b	4a
Empirical formula	$C_{26}H_{26}F_6N_4O_{10}S_2Zn$	$C_{23}H_{26}F_6N_6O_9S_2Z_n$	$C_{29}H_{30}F_6N_6O_9S_2Zn$	$C_{24}H_{23}F_6N_6O_{10}S_2Zn$
Formula weight	795.40	773.99	850.08	798.97
Temperature/K	200(2)	173(2)	200(2)	200(2)
Wavelength/Å	0.71073	0.71073	0.71073	0.71073
Crystal system	Orthorhombic	Triclinic	Monoclinic	Triclinic
Space group	$P2(1)2(1)2(1)$	$P\bar{1}$	$P2_1$	$P\bar{1}$
a/Å	10.2466(6)	12.6143(3)	10.0788(5)	8.4599(9)
b/Å	15.8966(9)	15.3304(4)	18.2874(9)	11.5955(13)
c/Å	20.5963(12)	16.6834(5)	10.6961(5)	17.874(2)
α/°		88.729(1)		77.059(2)
β/°		85.837(1)	116.558(1)	86.195(2)
γ/°		75.5869(1)		79.890(2)
Volume/Å^3	3354.9(3)	3116.45(14)	1763.43(15)	1681.6(3)
Z	4	4	2	2
Absorption coefficient/mm^{-1}	0.947	1.017	0.907	0.947
F(000)	1619	1576	868	810
Crystal size/mm^3	0.2 × 0.2 × 0.45	0.30 × 0.30 × 0.25	0.2 × 0.2 × 0.4	0.15 × 0.05 × 0.05
Reflections collected/unique	24009/8115	19369/10945	18362/8343	18591/8144
Refinement method	Based on F^2	Based on F^2	Based on F^2	Based on F^2
Data/restraints/parameters	8115/0/593	10945/2/851	8343/1/495	8144/0/567
Final *R* indices [$I > 2\sigma(I)$]	$R1 = 0.0597$	$R1 = 0.0607$	$R1 = 0.0270$	$R1 = 0.0605$
	$wR2 = 0.1675$	$wR2 = 0.1547$	$wR2 = 0.0631$	$wR2 = 0.1346$
R indices (all data)	$R1 = 0.0844$	$R1 = 0.1444$	$R1 = 0.0302$	$R1 = 0.1618$
	$wR2 = 0.1806$	$wR2 = 0.1985$	$wR2 = 0.0643$	$wR2 = 0.1624$

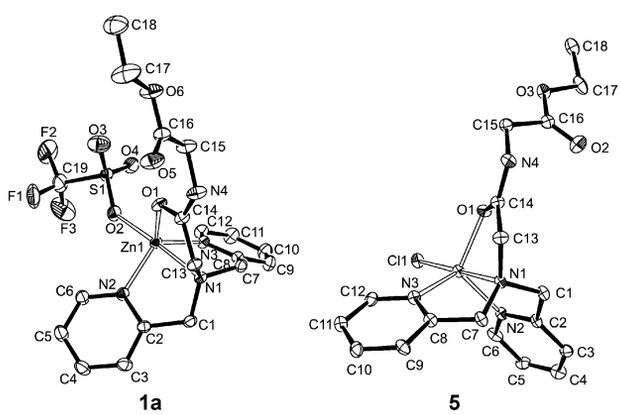

Fig. 1 Ortep[54] plots (30% ellipsoids) of the trigonal-bipyramidal cations of **1a** and **5**.

atom is localized at the fifth coordination site with 100% occupation. The axialy coordinated triflate ion is completed by a CF_3SO_2 unit with occupation factors of 57% for the carbon, fluorine, sulfur, and oxygen atoms, respectively. Accordingly, another triflate ion with occupation factors of 43% for each atom is found in the unit cell which belongs to the cocrystallized complex **2b**. Finally, the unit cell contains a disordered non-coordinating triflate ion and a non-coordinating water molecule with 43% occupation for its oxygen atom.

The first coordination sphere of **1b** is nearly trigonal-bipyramidal. Its N1–Zn–O(triflate) bond angle is 178° which is practically identical with those of the triflate complex **1a** and the chloro complex **5**. It should be noted that the geometry of **1b** may appear somewhat obscured in the X-ray structure analysis due to the overlapping hydroxo and triflato ligands. Similar effects have been discussed in much detail by Parkin and his coworkers.[32–35] However, the reasonable agreement between **1a**, **1b**, and **5** justifies the arguments presented below.

While the N1–Zn–O(Cl) angles in the triflato and chloro complexes are almost perfectly linear, a small bending is observed in the aquo complex **2b** which exhibits a value of 170°.

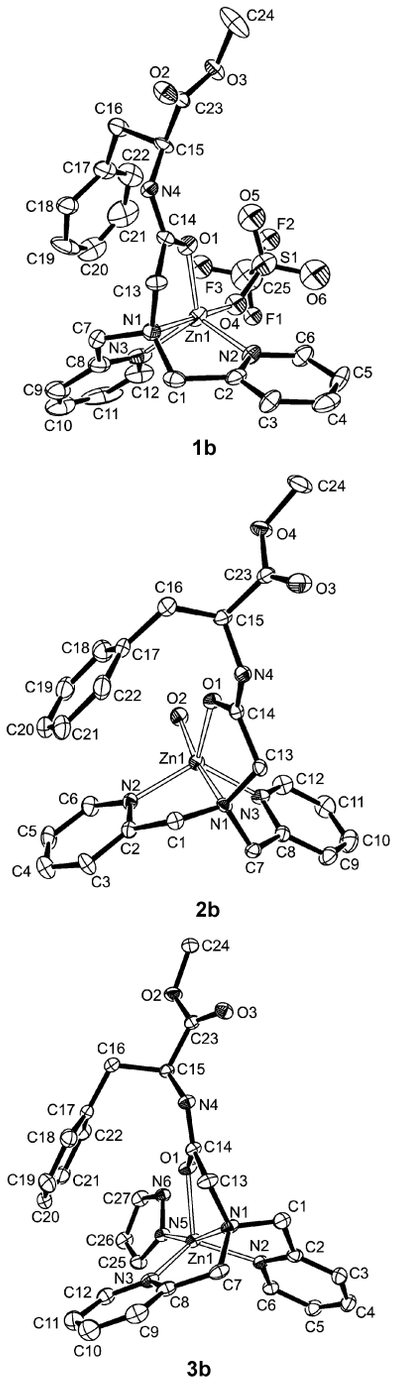

Fig. 2 Ortep plots (30% ellipsoids) of the trigonal-bipyramidal cations of **1b**, **2b**, and **3b**.

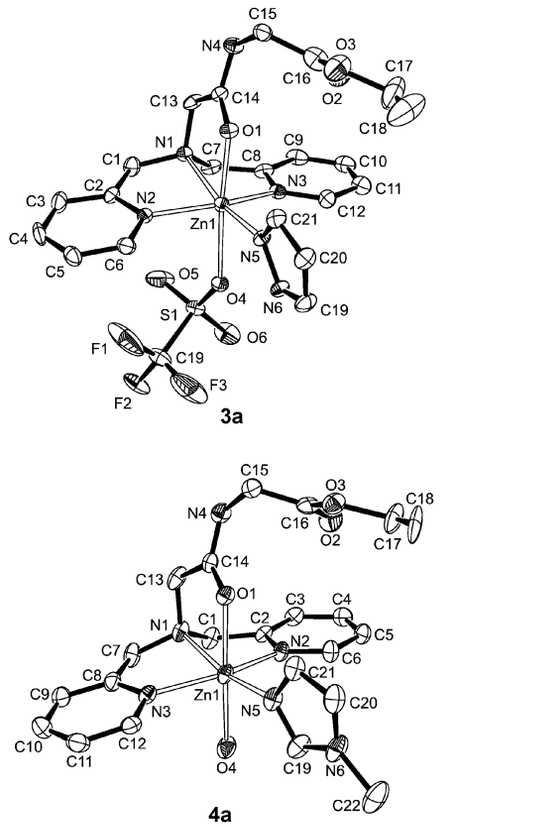

Fig. 3 Ortep plots (30% ellipsoids) of the octahedral cations of **3a** and **4a**.

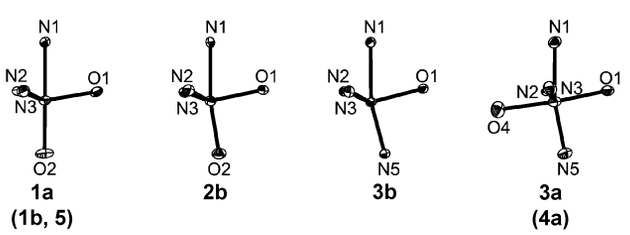

Fig. 4 Transition from trigonal-bipyramidal to octahedral structures.

This bending is even more pronounced in the pyrazole complex **3b** where the axial angle is 165°. Fig. 4 illustrates how the axial ligand moves towards the amide oxygen atom in the sequence **1a/1b/5** ≥ **2b**≥ **3b**. Also evident is an elongation of the Zn–N1 bond in the structure of **3b** (2.26 Å) compared with **1a**, **1b**, and **2b** (*ca*. 2.20 Å). The distances and angles defined by the atoms Zn, N1, O1, and N5 as observed for **3b** are invariant upon coordination of a sixth ligand in **3a** and **4a**. Most important, the N1–Zn–N(pz) (**3a**, 168°) and N1–Zn–N(*N*-Meim) (**4a**, 168°) angles show the same characteristic bending described above. Only a small breathing motion of the pyridine nitrogen atoms N2 and N3 is required to accommodate the respective incoming triflate (**3a**) and aquo (**4a**) ligands. An increase of the N2–Zn–N3 angle from *ca*. 120° in **3b** to *ca*. 153° in **3a** and **4a** is observed.

An important feature in the structures containing the phenylalanine moiety is the orientation of their amino acid side chains. In **1b**, **2b**, and **3b** (Fig. 3), respectively, the benzyl substituent is located between one of the pyridine rings and the coordinating amide function. It always points towards the fifth "active" coordination site. The distances between the zinc ion and the center of the phenyl ring are 4.2 Å (**1b**), 4.5 Å (**2b**), and 4.3 Å (**3b**), respectively.

Discussion

The starting point for our investigations was the question whether bpaAc–Phe–OMe can stabilize five-coordinate zinc complexes by aromatic interactions involving its non-coordinating benzyl group. In order to answer this question we were looking for structurally characterized zinc complexes in which the coordination sphere is clearly affected by the aromatic side chain. The first examples are provided by the pyrazole and *N*-methylimidazole complexes **3b** and **4b**. This is revealed by comparison with the corresponding bpaAc–Gly–OMe complexes **3a** and **4a**, as well as with zinc complexes of other tripodal ligands derived from trispicolylamine by replacement of one pyridine ring by another donor (O, S, or aliphatic amine).

It is well documented that without any stabilizing effects provided by the tripodal ligand framework the geometry of

such complexes depends on the monodentate coligand *trans* to the central amine. Halide ions[16,17,31,36] and anionic oxygen donor ligands such as benzoate[31] and phosphate mono-[37] and di-esters[17,38] always form distorted trigonal-bipyramidal complexes. In contrast, the only published structure of an imidazole complex $[(dpg)(im)(H_2O)Zn]^+$ is octahedral (dpg = dipicolylglycine).[38] In its corresponding 2-methylimidazole analogue $[(dpg)Zn(2\text{-}Meim)]^+$ a trigonal-bipyramidal geometry is enforced by the steric demand of the 2-methyl substituent. This structure can therefore not be compared. Our bpa–Gly–OEt complexes confirm the trends reported in the literature. Triflato and chloro ligands occupy the axial position of a trigonal-bipyramid whereas distorted octahedral geometries are induced by pyrazole and N-methylimidizazole. This preference for six-coordination is so strong that in the absence of additional water a weakly coordinating triflate ion is bound in **3a**. It is interesting to note that the similarity between **3a** and **4a** clearly excludes hydrogen bonding as a stabilizing geometric factor.

It is evident that a significant stabilizing effect is required in order to overcome the tendency of pyrazole or *N*-methylimidazole to give only octahedral zinc complexes. This is provided by the ligand bpaAc–Phe–OMe which exclusively yields trigonal-bipyramidal structures. Its pyrazole complex **3b** contains the heterocyclic coligand *trans* to the bridgehead nitrogen atom N1. This position is also characteristic for the octahedral complexes **3a** and **4a**. However, **3b** does not bind an additional ligand, water or triflate ion. Two types of intramolecular aromatic interactions may explain this behavior. (1) A π-cation attraction exists between the phenyl ring and the divalent zinc ion. These are long range electrostatic charge–quadrupole interactions[39,40] which are of paramount importance in biological receptors.[41] Gallivan and Dougherty have demonstrated that in proteins they are active up to distances of more than 6 Å.[42] In our complexes the Zn–Ph distances are *ca.* 4.5 Å. This excludes covalent contributions but is well within the range of π-cation attractions. (2) An additional stabilization may result from intramolecular π–π interactions. The CH(6) proton of the phenyl ring is located *ca.* 3.8 Å above the nearest pyridine ring center. The relative orientation of the two rings is best described as distorted T-shaped. Edge-to-face or T-shaped arrangements are commonly observed in non-covalently bound arene structures such as crystalline benzene, metal complexes, or proteins.[43,44]

It is a feature of our design that bpaAc–Phe–OMe forms aromatic interactions only in trigonal-bipyramidal complexes. This is revealed by a comparison with X-ray structures of the related square-pyramidal copper complexes $[(bpaAc–Phe–OMe)Cu(Cl)]^+$ and $[(bpaAc–Phe–OMe)(CH_3CN)Cu]^{2+}$.[28] In both compounds we have observed two superimposed geometries with the phenyl ring pointing either towards or away from the metal center. This structural feature indicates that the benzyl side chain is highly flexible and that no significant interaction exists between the amino acid side chain and the copper(II) ion. The closest Cu–Ph(center) distance is 7.24 Å which is *ca.* 3 Å longer than in the zinc complexes **1b**, **2b**, and **3b**.

In addition to the stabilization of trigonal-bipyramidal zinc complexes by aromatic interactions a second interesting aspect appears in our data. The fact that X-ray structures usually represent minima on an energy hyperpotential surface has been exploited for the description of mechanistic pathways by the structure correlation method.[45–49] Our complexes map a well defined transition from trigonal-bipyramidal to octahedral structures in zinc complexes. This is illustrated in Fig. 4. The reaction path consists of two motions. In the series **1a/1b/5** to **2b** to **3b** the axial ligand bends towards the amide oxygen donor. The structure of **3b** represents a tense state which is pre-organized to bind an additional ligand and form a distorted octahedral complex. This is accomplished by a small motion of the two pyridine ligands in order to accommodate the sixth incoming ligand.

Conclusions

With our study we have demonstrated that weak non-covalent interactions involving aromatic amino acid side chain functional groups can be used to tune the stereochemistry of zinc complexes. It was thereby possible to stabilize the unusual five-coordinate geometry of the pyrazole complex **3b**. This compound possesses an interesting tense structure which represents an intermediate in the reaction pathway for trigonal-bipyramidal to octahedral complexes. Having a series of related crystal structures we were able to propose the first plausible reaction trajectory for this important stereochemical transition.

Experimental

General methods

Spectra were recorded with the following instruments: IR: Mattson Polaris FT IR; ^{1}H- and ^{13}C-NMR: Bruker Avance DPX 300. All chemical shifts are referenced to TMS as internal standard, with high frequency shifts recorded as positive. The assignment of ^{1}H-NMR signals was assisted by ^{1}H–^{1}H and ^{1}H–^{13}C COSY spectra. All reactions were carried out under an atmosphere of dry nitrogen. The following workup was performed under ambient laboratory conditions unless stated otherwise. The ligands bpaAc–Gly–OEt and bpaAc–Phe–OMe, as well as the complex salts $[(bpaAc–Gly–OEt)Zn(OTf)](OTf)$ (**1a**) (OTf = SO_3CF_3), $[(bpaAc–Gly–OEt)Zn(H_2O)](OTf)$ (**2a**), $[(bpaAc–Phe–OMe)Zn(OTf)](OTf)$ (**1b**) and $[(bpaAc–Phe–OMe)Zn(H_2O)](OTf)_2$ (**2b**) were prepared as described elsewhere.[26] The synthesis and crystal structure of $[(bpaAc–Gly–OEt)Zn(Cl)]_2[ZnCl_4]$ (**5**) has also been reported earlier.[27] Absolute solvents (CH_2Cl_2, Et_2O, CH_3CN) were purchased from Fluka and stored under nitrogen. Ethyl acetate was reagent grade (Roth). All solvents were used without further purification. All other chemicals and deuterated solvents were obtained from Aldrich.

[(bpaAc–Gly–OEt)Zn(pz)(OTf)](OTf) (3a)

The complex **3a** was synthesized by two different methods. In one case solid $Zn(OTf)_2$ was added to an equimolar solution of bpaAc–Gly–OEt in acetonitrile. One equivalent of solid pyrazole was added after 15 min with stirring. The other method started from $[(bpaAc–Gly–OEt)Zn(OTf)](OTf)$ (**1a**). Both procedures afforded the product. However, the first method yielded the compound as an oil which separated from the reaction solution. On that account the second pathway is preferable and therefore described in more detail below.

$[(bpaAc–Gly–OEt)Zn(OTf)](OTf)\cdot H_2O$ (377.8 mg, 0.52 mmol) was dissolved with stirring in 10 ml acetonitrile. Solid pyrazole (35.4 mg, 0.52 mmol) was added and stirring continued overnight at RT. After removal of all solvent in a vacuum the crude product was treated with 5 ml of CH_2Cl_2. The solution was stored at −20 °C and filtrated in order to remove all insoluble material. After addition of some drops of Et_2O and storing at −20 °C a small fraction of a yellow oil deposited. The supernatant was decanted and stored in a refrigerator at 4 °C. Repeated addition of Et_2O afforded the product as a colorless crystaline solid (280 mg, 0.36 mmol, 69%). Some crystals were suitable for an X-ray structure analysis. $C_{23}F_6H_{26}N_6O_9S_2Zn$ (774.0 g mol^{-1}): calc. C 35.69, H 3.39, N 10.86; found C 35.80, H 3.54, N 10.87%. FAB-MS (nitrobenzyl alcohol): *m*/*z* = 555 ([(bpaAc–Gly–OEt)Zn(OTf)]$^+$), 405 ([(bpaAc–Gly–OEt)Zn]$^+$). ^{1}H NMR (300 MHz, $CDCl_3$), δ [ppm] = 1.14 (t, $^3J_{HH}$ = 7.1 Hz, 3H, OCH_2CH_3); 3.80 (d, $^3J_{HH}$ = 5.7 Hz, 2H, $^{\alpha}CH_2$); 3.90 (s, 2H, C(O)–CH_2); 4.02

(q, $^3J_{HH}$ = 7.1 Hz, 3H, OCH_2CH$_3$); 4.54 (s, 4H, 2 × py-CH$_2$); 6.75 (s, br, 1H, H4-pz); 7.41 (m, 2H, 2 × H5-py); 7.53 (d, $^3J_{HH}$ = 7.7 Hz, 2H, 2 × H3-py); 7.82 (d, $^3J_{HH}$ = 5.1 Hz, 2H, 2 × H6-py); 7.97 (m, 2H, 2 × H4-py); 8.12 (s, br, 2H, H3-pz + H5-pz); 8.82 (t, $^3J_{HH}$ = 5.4 Hz, 1H, NH); 13.13 (−20 °C, 1H, NH-pz). IR (KBr): $\bar{\nu}$ = 1754, 1729 (CO$_2$Et), 1651 (amide I), 1281, 1252 (OTf) cm^{-1}.

[(bpaAc–Gly–OEt)Zn(*N*-Meim)(H$_2$O)](OTf)$_2$ (4a)

The complex **4a** can be obtained either from Zn(OTf)$_2$ or from **1a**. Both methods work equally well in this case. We describe the first route below.

Zn(OTf)$_2$ (461.7 mg, 1.27 mmol) was added in one portion to a stirred solution of bpaAc–Gly–OEt (435.1 mg, 1.27 mmol) in 15 ml of acetonitrile. *N*-Methylimidazole (104.3 mg, 1.27 mmol) was added and stirring was continued overnight at RT. After removal of all solvent the solid residue was treated with 15 ml of CH_2Cl_2. The mixture was cooled to −20 °C and filtered to yield a colorless solution. All solvent was removed and the crude product dried in a vacuum for several hours. The solid residue was then redissolved in a minimum of hot ethyl acetate using an ultrasound bath. Upon storage at −20 °C for several days **4a** precipitated as a colorless solid precipitate which was collected on a sintered-glass filter and dried under vacuum (577.7 mg, 0.72 mmol, 57%). Recrystallization from ethyl acetate by slow evaporation of the solvent afforded colorless crystals which were suitable for an X-ray structure analysis. $C_{24}H_{30}F_6N_6O_{10}S_2Zn$ (806.0 g mol^{-1}): calc. C 35.76, H 3.75, N 10.43; found C 35.79, H 3.89, N 10.22%. FAB-MS (nitrobenzyl alcohol): *m*/*z* = 637 ([(bpaAc–Gly–OEt)(Meim)Zn(OTf)]$^+$); 555 ([(bpaAc–Gly–OEt)Zn(OTf)]$^+$); 405 ([(bpaAc–Gly–OEt)Zn]$^+$). ^{1}H NMR (300 MHz, $CDCl_3$), δ [ppm] = 1.12 (t, 3H, $^3J_{HH}$ = 7.1 Hz, OCH$_2$CH_3); 2.31 (s, br, H$_2$O); 3.75 (d, $^3J_{HH}$ = 5.6 Hz, 2H, $^{\alpha}$CH$_2$); 3.82 (s, 2H, C(O)–CH$_2$); 3.95 (s, 3H, N–CH$_3$); 4.00 (q, 2H, $^3J_{HH}$ = 7.1 Hz, OCH_2CH$_3$); 4.47, 4.60 (2 × d, $^2J_{HH}$ = 15.7 Hz, 4H, 2 × py-CH$_2$); 7.25 (m, 1H, H4-im); 7.37–7.52 (m, 5H, 2 × H3-py + 2 × H5-py + 1 × H5-im); 7.93 (m, 4H, 2 × H4-py + 2 × H6-py); 8.36 (s, 1H, H2-im); 8.67 (t, $^3J_{HH}$ = 5.4 Hz, 1H, NH). IR (KBr): $\bar{\nu}$ = 1750 (CO$_2$Et); 1649 (amide I); 1279 (CF_3SO_3) cm^{-1}.

[(bpaAc–Phe–OMe)Zn(pz)](OTf)$_2$ (3b)

As in the case of **4a**, both methods described above worked equally well in the synthesis of **3b**. The procedure starting from a mixture of Zn(OTf)$_2$, bpaAc–Phe–OMe, and pyrazole is described below.

Zn(OTf)$_2$ (441.7 mg, 1.22 mmol) was added in one portion to a stirred solution of bpaAc–Phe–OMe (509.1 mg, 1.22 mmol) in 15 ml of acetonitrile. After 15 min, pyrazole (82.7 mg, 1.22 mmol) was added and stirring was continued overnight at RT. After removal of all solvent in a vacuum the residual solid was treated with 15 ml of CH_2Cl_2. The mixture was cooled to −20 °C and filtered in order to remove all insoluble impurities and starting materials. The volume of the filtrate was reduced to *ca.* 1/2 and a few drops of diethyl ether were added. Storage of the solution at −20 °C and repeated addition of Et$_2$O afforded the product as a white, hygroscopic precipitate (562.5 mg, 0.66 mmol, 54%). The product was collected on a sintered-glass filter under dry nitrogen and dried under vacuum. The compound is extremely hygroscopic and C,H,N elemental analysis data suggest the presence of water in all bulk samples we obtained. Suitable crystals for an X-ray structure analysis were obtained by recrystallization of the product from CH_2Cl_2–Et$_2$O at −20 °C under an atmosphere of dry nitrogen. $C_{29}H_{30}F_6N_6O_9S_2Zn{\cdot}H_2O$ (868.1 g mol^{-1}): calc. C 40.12, H 3.72, N 9.68; found C 40.54, H 3.67, N 9.55%. FAB–MS (nitrobenzyl alcohol): *m*/*z* = 631 ([(bpaAc–Phe–OMe)Zn(OTf)]$^+$); 481 ([(bpaAc–Gly–OEt)Zn]$^+$). ^{1}H NMR (300 MHz, $CDCl_3$), δ [ppm] = 2.85 (ABX, $^2J_{HH}$ = 13.9 Hz, $^3J_{HH}$ = 9.3 Hz, 1H, $^{\beta}$CH$_2$); 3.04 (ABX, $^2J_{HH}$ = 13.9 Hz, $^3J_{HH}$ = 5.8 Hz, 1H, $^{\beta}$CH$_2$); 3.50 (s, 3H, OCH$_3$); 3.78, 3.88 (2 × d, $^2J_{HH}$ = 18.0 Hz, 2H, C(O)–CH$_2$); 4.39 (m, 5H, $^{\alpha}$CH + 2 × py-CH$_2$); 6.73 (m, 1H, H4-pz); 6.97 (m, 1H, H4-Ph); 7.06 (m, 4H, H2,3,5,6-Ph); 7.39 (m, br, 2H, 2 × H5-py); 7.50 (m, 2H, 2 × H3-py); 7.77 (m, br, 2H, 2 × H6-py); 7.95 (m, 2H, 2 × H4-py); 8.06 (m, 2H, H3-pz + H5-pz); 8.91 (d, $^3J_{HH}$ = 7.1 Hz, 1H, NH); 13.00 (only observed at or below −20 °C, 1H, NH-pz). IR (KBr): $\bar{\nu}$ = 1749 (CO$_2$Me); 1638 (amide I); 1281, 1248 (CF_3SO_3) cm^{-1}.

[(bpaAc–Phe–OMe)Zn(*N*-Meim)](OTf)$_2$ (4b)

The synthesis of **4b** has to be started from [(bpaAc–Phe–OMe)Zn(OTf)](OTf) (**1b**). No product was obtained from stoichiometric mixtures of Zn(OTf)$_2$, bpaAc–Phe–OMe, and *N*-methylimidazole.

N-Methylimidazole (37 μl, 0.47 mmol) was added in one portion to a stirred solution of [(bpaAc–Phe–OMe)-Zn(H$_2$O)](OTf)$_2$ (375 mg, 0.47 mmol) in 15 ml of acetonitrile. Stirring was continued overnight at RT. After removal of all solvent in a vacuum the residual solid was dissolved in CH_2Cl_2 and treated with Et$_2$O. After storing at −20 °C and repeated addition of Et$_2$O a yellow oil deposited. The supernatant was decanted and the oil dried under a vacuum. The product was obtained as a weak yellow foam (217 mg, 0.25 mmol, 53%). $C_{30}H_{32}F_6N_6O_9S_2Zn$ (864.1 g mol^{-1}): calc. C 41.70, H 3.73, N 9.73; found C 41.70, H 3.82, N 9.41%. FAB-MS (nitrobenzyl alcohol): *m*/*z* = 631 ([(bpaAc–Phe–OMe)Zn(OTf)]$^+$); 481 ([(bpaAc–Gly–OEt)Zn]$^+$). ^{1}H NMR (300 MHz, $CDCl_3$), δ [ppm] = 2.81 (ABX, $^2J_{HH}$ = 13.7 Hz, $^3J_{HH}$ = 9.3 Hz, 1H, $^{\beta}$CH$_2$); 3.02 (ABX, $^2J_{HH}$ = 13.7 Hz, $^3J_{HH}$ = 5.9 Hz, 1H, $^{\beta}$CH$_2$); 3.49 (s, 3H, OCH$_3$); 3.71, 3.80 (2 × d, $^2J_{HH}$ = 17.4 Hz, 2H, C(O)–CH$_2$); 3.94 (s, 3H, N-CH$_3$); 4.38 (m, 5H, $^{\alpha}$CH + 2 × py-CH$_2$); 6.98 (m, 1H, H4-Ph); 7.05 (m, 4H, H2,3,5,6-Ph); 7.26 (s, br, 1H, H4-im); 7.43 (m, 5H, 2 × H3-py + 2 × H5-py + H5-im); 7.92 (m, 4H, 2 × H4-py + 2 × H6-py); 8.29 (s, br, 1H, H2-im); 8.74 (d, $^3J_{HH}$ = 7.3 Hz, 1H, NH). IR (KBr): $\bar{\nu}$ = 1748 (CO$_2$Me); 1642 (amide I); 1280, 1260, (CF_3SO_3) cm^{-1}.

X-Ray data collection and structure refinement details

Crystal data and experimental conditions are listed in Table 2. The molecular structures are illustrated in Figs. 1, 2, and 3. Selected bond lengths and bond angles with standard deviations in parentheses are summarized in Table 1.

Intensity data were collected with graphite monochromated Mo-Kα radiation, on a SMART 1000 CCD-diffractometer (**1b**, **3b**, **4a**), and on a Nonius KappaCCD area detector (**3a**) (exposure time: 10 s per frame, $\Delta\omega$ = 0.3°). The collected reflections were corrected for Lorentz, polarization, and absorption effects.[50] All structures were solved by direct methods and refined by full matrix least squares methods on F^2.[51–53] Non-hydrogen atoms were refined with anisotropic thermal parameters. Hydrogen atoms were calculated for idealized geometries and allowed to ride on their preceding atoms with isotropic displacement parameters tied to those of the adjacent atoms by a factor of 1.5.

CCDC reference numbers 137192, 137193, 171339 and 173038.

See http://www.rsc.org/suppdata/dt/b2/b204125c/ for crystallographic data in CIF or other electronic format.

Acknowledgements

The authors gratefully acknowledge financial support from the Deutsche Forschungsgemeinschaft. We thank Prof. Rudi van Eldik who generously let us share his equipment, laboratory space, and funding.

References

1 B. L. Vallee and R. J. P. Williams, *Proc. Natl. Acad. Sci. USA*, 1968, **59**, 498.
2 P. Comba, *Coord. Chem. Rev.*, 2000, **200–202**, 217–245.
3 C. Ochs, F. E. Hahn and T. Lugger, *Eur. J. Inorg. Chem.*, 2001, 1279–1285.
4 M. Schatz, M. Becker, F. Thaler, F. Hampel, S. Schindler, R. R. Jacobson, Z. Tyeklar, N. N. Murthy, P. Ghosh, Q. Chen, J. Zubieta and K. D. Karlin, *Inorg. Chem.*, 2001, **40**, 2312.
5 M. Pascaly, M. Duda, F. Schweppe, K. Zurlinden, F. K. Muller and B. Krebs, *J. Chem. Soc., Dalton Trans.*, 2001, 828.
6 A. von Zelewsky, *Coord. Chem. Rev.*, 1999, **190–192**, 811.
7 E. A. Ambundo, M. V. Deydier, A. J. Grall, N. Aguera-Vega, L. T. Dressel, T. H. Cooper, M. J. Heeg, L. A. Ochrymowycz and D. B. Rorabacher, *Inorg. Chem.*, 1999, **38**, 4233.
8 L. F. Szczepura, L. M. Witham and K. J. Takeuchi, *Coord. Chem. Rev.*, 1998, **174**, 5.
9 S. Schindler, *Eur. J. Inorg. Chem.*, 2000, 2311.
10 A. Abufarag and H. Vahrenkamp, *Inorg. Chem.*, 1995, **34**, 3279.
11 T. Okuno, S. Ohba and Y. Nishida, *Polyhedron*, 1997, **16**, 3765.
12 S. Ito, S. Nishino, H. Itoh, S. Ohba and Y. Nishida, *Polyhedron*, 1998, **17**, 1637.
13 T. Kobayashi, T. Okuno, T. Suzuki, M. Kunita, S. Ohba and Y. Nishida, *Polyhedron*, 1998, **17**, 1553.
14 C. Policar, S. Durot, F. Lambert, M. Cesario, F. Ramiandrasoa and I. Morgenstern-Badarau, *Eur. J. Inorg. Chem.*, 2001, 1807.
15 Y. Nishida and K. Takahashi, *Inorg. Chem.*, 1988, **27**, 1406.
16 R. Burth, A. Stange, M. Schäfer and H. Vahrenkamp, *Eur. J. Inorg. Chem.*, 1998, 1759.
17 A. Trösch and H. Vahrenkamp, *Eur. J. Inorg. Chem.*, 1998, 827.
18 L. M. Berreau, M. M. Makowska-Grzyska and A. M. Arif, *Inorg. Chem.*, 2000, **39**, 4390.
19 G. Parkin, *Chem. Commun.*, 2000, 1971.
20 R. Alsfasser, S. Trofimenko, A. Looney, G. Parkin and H. Vahrenkamp, *Inorg. Chem.*, 1991, **30**, 4098.
21 A. Looney, G. Parkin, R. Alsfasser, M. Ruf and H. Vahrenkamp, *Angew. Chem.*, 1992, **104**, 57.
22 M. Ruf and H. Vahrenkamp, *Inorg. Chem.*, 1996, **35**, 6571.
23 K. Ogawa, K. Nakata and K. Ichikawa, *Chem. Lett.*, 1998, 797.
24 A. Trösch and H. Vahrenkamp, *Inorg. Chem.*, 2001, **40**, 2305.
25 E. Kimura, T. Koike and K. Toriumi, *Inorg. Chem.*, 1988, **27**, 3687.
26 N. Niklas, O. Walter and R. Alsfasser, *Eur. J. Inorg. Chem.*, 2000, 1723.
27 N. Niklas, S. Wolf, G. Liehr, C. E. Anson, A. K. Powell and R. Alsfasser, *Inorg. Chim. Acta*, 2001, **314**, 126.
28 N. Niklas, F. Hampel, O. Walter, G. Liehr and R. Alsfasser, *Eur. J. Inorg. Chem.*, 2002, 1839.
29 J. Glerup, P. A. Goodson, D. J. Hodgson, K. Michelsen, K. M. Nielsen and H. Weihe, *Inorg. Chem.*, 1992, **31**, 4611.
30 Z. W. Mao, Q. W. Hang, W. X. Tang, S. X. Liu, Z. M. Wang and J. L. Huang, *Polyhedron*, 1996, **15**, 321.
31 H. Adams, N. A. Bailey, D. E. Fenton and Q.-Y. He, *J. Chem. Soc., Dalton Trans.*, 1997, 1533.
32 K. Yoon and G. Parkin, *J. Am. Chem. Soc.*, 1991, **113**, 8414.
33 K. Yoon and G. Parkin, *Inorg. Chem.*, 1992, **31**, 1656.
34 G. Parkin, *Acc. Chem. Res.*, 1992, **25**, 455.
35 G. Parkin, *Chem. Rev.*, 1993, **93**, 887.
36 C. S. Allen, C.-L. Chuang, M. Cornebise and J. W. Canary, *Inorg. Chim. Acta*, 1995, **239**, 29.
37 H. Adams, N. A. Bailey, D. E. Fenton and Q.-Y. He, *J. Chem. Soc., Dalton Trans.*, 1995, 697.
38 A. Abufarag and H. Vahrenkamp, *Inorg. Chem.*, 1995, **34**, 2207.
39 S. Mecozzi, A. P. West and D. A. Dougherty, *J. Am. Chem. Soc.*, 1996, **118**, 2307.
40 S. L. De Wall, E. S. Meadows, L. J. Barbour and G. W. Gokel, *Proc. Natl. Acad. Sci. USA*, 2000, **97**, 6271.
41 J. C. Ma and D. A. Dougherty, *Chem. Rev.*, 1997, **97**, 1303.
42 J. P. Gallivan and D. A. Dougherty, *Proc. Natl. Acad. Sci. USA*, 1999, **96**, 9459.
43 C. A. Hunter and J. K. M. Sanders, *J. Am. Chem. Soc.*, 1990, **112**, 5525.
44 C. Janiak, *J. Chem. Soc., Dalton Trans.*, 2000, 3385.
45 E. L. Muetterties and L. J. Guggenberger, *J. Am. Chem. Soc.*, 1974, **96**, 1748.
46 H.-B. Bürgi and J. D. Dunitz, *Structure Correlation*, VCH, Weinheim, 1993.
47 T. Auf der Heyde, *Angew. Chem.*, 1994, **106**, 871.
48 H. Vahrenkamp, *Acc. Chem. Res.*, 1999, **32**, 589.
49 M. Rombach, C. Maurer, K. Weis, E. Keller and H. Vahrenkamp, *Chem. Eur. J.*, 1999, **5**, 1013.
50 (*a*) A. C. T. North, D. C. Phillips and F. S. Mathews, *Acta Crystallogr., Sect. A*, 1968, **24**, 351; (*b*) Collect, data collection software, Nonius B.V., The Netherlands, 1998; (*c*) Scalepack, data processing software, Z. Otwinowski and W. Minor, *Methods Enzymol.*, 1997, **276**, 307.
51 A. Altomare, G. Cascarano, C. Giacovazzo and A. Guagliardi, *J. Appl. Crystallogr.*, 1993, **26**, 343–350.
52 G. M. Sheldrick, SHELXTL-PC, Siemens Analytical X-Ray Instruments Inc., Madison, WI, USA, 1994.
53 G. M. Sheldrick, SHELXL-97, Universität Göttingen, Germany, 1997.
54 M. N. Burnett and C. K. Johnson, Ortep, Report ORNL-6895, Oak Ridge National Laboratory, Oak Ridge, TN, USA, 1996.